JOURNAL OF AIRCRAFT
Vol. 47, No. 3, May–June 2010

Engineering Notes

Optimization of Hover-to-Cruise Transition Maneuver Using Variable-Incidence Wing

Adnan Maqsood* and Tiauw Hiong Go†
Nanyang Technological University, Singapore 639798, Republic of Singapore

DOI: 10.2514/1.44453

Nomenclature

A	=	disc area of the propeller
D	=	drag
g	=	acceleration due to gravity
J	=	cost/objective function
L	=	lift
L/W	=	lift-to-weight ratio
m	=	mass of the aircraft
T	=	thrust
$T_{\max}$	=	maximum thrust
T/W	=	thrust-to-weight ratio
$(T/W)_{\max}$	=	maximum thrust-to-weight ratio
u	=	horizontal velocity
$\mathbf{u}$	=	control variable vector
u_t	=	terminal horizontal velocity
V	=	freestream velocity
w_i	=	ith weight coefficient
v_t	=	terminal vertical velocity
W	=	weight
w	=	induced velocity aft of the propeller
$\ddot{x}$	=	horizontal acceleration
y_i	=	altitude at ith discretized calculation instant
$\ddot{z}$	=	vertical acceleration
α_{fus}	=	fuselage and inboard wing angle of attack
α_{prop}	=	angle of attack of the propeller
α_{wing}	=	outboard wing angle of attack
$\dot{\alpha}_{\text{wing}}$	=	rate of change of outboard wing angle of attack
γ	=	flight-path angle
ρ	=	air density
$\dot{(\bullet)}$	=	rate of change of variable $(\bullet)$, $\equiv \frac{\mathrm{d}}{\mathrm{d}t}(\bullet)$

I. Introduction

IN ORDER to enhance the flight envelope of unmanned air vehicles (UAVs), there have been efforts to combine the hover capabilities of rotorcraft with the endurance and speed capabilities of fixed-wing aircraft [1]. Such efforts have led to a type of agile aircraft that can perform hover, coupled with efficient flight during forward cruise. Such a vehicle is said to have a convertible configuration. An inherent problem for such vehicles is the transition maneuver between forward flight (primary flight modality) and hover (secondary flight modality), which usually exhibits the following issues: 1) significant altitude variations, 2) long transition times, 3) large control effort, 4) high thrust-to-weight ratio requirement, and 5) loss of partial control.

These characteristics are undesirable and reduce the maneuver potential of the vehicle in tight spaces. The seminal work for the transition phenomenon involving a simple-ducted-fan-with-wings UAV can be attributed to Nieuwstadt and Murray [2]. The investigation encompasses a hover-to-cruise transition of a 0.5 kg vehicle in 6 s. The authors noted altitude loss during the transition but did not quantify the relevant performance parameters. Other prominent contributions in this area (e.g., [3–8]) mostly focus on achieving transitions in a smooth manner with the help of an efficient controller. Very few studies have been conducted by adding necessary transition-assisting features on the vehicles in the improvements of transition maneuver performances. Aurora Flight Sciences [9] has used the torsionally-decoupled wings on its ducted-fan UAVs, which are said to help in the transition maneuver. Kubo and Suzuki [10] studied the utilization of slats and flaps for achieving optimized transitions. Their work does not consider thrust limitation, thus the optimized maneuver demands excessively high $(T/W)_{\max}$.

The study reported in this paper is part of an effort to find an efficient transition technique for small UAVs to achieve minimal variation in altitude using reasonable T/W requirements. Specifically, the feasibility of an aerodynamic-assisted transition technique using a variable-incidence wing is explored. A two-degree-of-freedom point-mass model with pitching constraints is used for the modeling of the aircraft dynamics. The aerodynamic-force-and-moment database, which is needed for the optimization study, is developed both in the prestall and poststall regimes using a three-dimensional vortex-lattice code. The performance obtained is then analyzed in comparison with the fixed-wing case.

II. Aerodynamic Modeling

For this study, aerodynamic forces and moments are computed using a commercial code called Multisurface Aerodynamics (MSA) [11]. MSA is based on the three-dimensional vortex-lattice method (VLM) and can predict the profile drag with good accuracy for arbitrary configurations. VLM is a well-established technique based on panel methods, which are derived from potential flow theory and provide inviscid aerodynamic calculations (see [12] for further details). Using the effective angles of attack along the wing span, as computed using VLM and the boundary-layer theory, the total profile drag can be calculated by integrating the incremental profile drag at various span locations. For the evaluation of the aerodynamic properties in the poststall regime, the numerical code works using the same boundary-layer approximation technique for the calculation of the transition and separation points.

The longitudinal dynamics are assumed to be decoupled from the lateral–directional motions; thus, only the longitudinal aerodynamic forces and moments are computed. This assumption simplifies the modeling and is sufficient to capture the essential behavior of the hover-to-cruise transition maneuver.

A. Description of the Aircraft Model

Figure 1 shows the UAV platform considered, which has a conventional wing–tail configuration with a tractor-type propeller. The fuselage length, as well as the wing span, is 1 m. The aspect ratio (AR) of the wing is 4.31. Typical dimensional attributes of the model include a rectangular wing with a mean aerodynamic chord of 0.2379 m and a propeller with a diameter of 0.254 m. The wing and

Received 18 March 2009; revision received 18 January 2010; accepted for publication 18 January 2010. Copyright © 2010 by Adnan Maqsood and Tiauw Hiong Go. Published by the American Institute of Aeronautics and Astronautics, Inc., with permission. Copies of this paper may be made for personal or internal use, on condition that the copier pay the $10.00 per-copy fee to the Copyright Clearance Center, Inc., 222 Rosewood Drive, Danvers, MA 01923; include the code 0021-8669/10 and $10.00 in correspondence with the CCC.

*Graduate Student, School of Mechanical and Aerospace Engineering. Student Member AIAA.

†Assistant Professor, School of Mechanical and Aerospace Engineering. Senior Member AIAA.

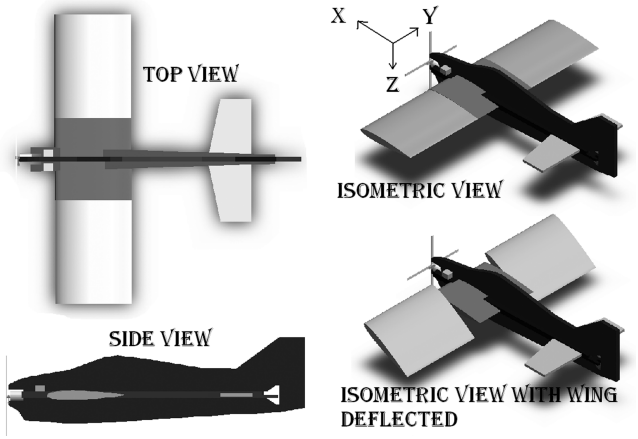

Fig. 1 Views of the UAV with variable-incidence wing.

the tail employ the NACA 0012 airfoil. The feature that differentiates this platform from the conventional one is the wing. It is divided into two sections: inboard and outboard. The inboard section (0.25 m span) is fixed with the fuselage, and it is submerged in the slipstream of the propeller. The outboard section, on the other hand, can be rotated about the wing's quarter-chord axis (called the variable-incidence wing feature).

B. Methodology for Aerodynamic Computation

Slipstream effects from the propeller are assumed conserved inside a stream tube, such that the panels submerged under its effects are isolated from the neighboring panels. The stream tube has approximately the same diameter as the propeller. Moreover, it is assumed that there is no contraction of the stream tube to maintain the flow momentum and, therefore, the diameter of the stream tube remains constant throughout the slipstream region of the aircraft. In this analysis, the fuselage, the fin, the inboard wing section, and the horizontal tail are assumed to be submerged in the propeller slipstream, whereas the outboard sections of the wing and the horizontal tail experience the freestream effects.

For the computation of aerodynamic forces within the slipstream, the span of the wing and horizontal tails is increased significantly, such that the effect of the three-dimensional complex vortex flows should not intrude the stream tube. The aerodynamic forces under the freestream effects are evaluated across the complete transition envelope, including the three-dimensional wing-tip vortices.

For the slipstream evaluation, the McCormick formulation [13] for free propellers, which can be expressed as a quartic equation as shown next, is used:

$$w^4 + 2V(\cos\alpha_{\text{prop}})w^3 + V^2w^2 = \left(\frac{T}{2\rho A}\right)^2 \tag{1}$$

At a particular thrust T, freestream airspeed V, and propeller's angle of attack (AOA) α_{prop}, Eq. (1) can be solved for the net-induced velocity w aft of the propeller. In Fig. 2, the lift and drag characteristics are plotted for the complete unpowered aircraft, such that the angle of incidence of the wing is equal to the aircraft AOA. In Fig. 2a, the lift is plotted against the range of the AOA from 0 to 90 deg for several airspeeds. The stall AOA in cruise conditions is about 22 deg, and the prestall data predict a fairly linear lift curve. The variation of drag with the AOA is plotted for several velocities in Fig. 2b. The conventional behavior of the increase in drag due to the increase in airspeed and AOA is observed. The aerodynamic forces of the outboard wing and the rest of the aircraft are computed separately, and they are added across a particular angle of incidence and airspeed for the variable-incidence case.

III. Optimal Hover-to-Cruise Transition

The transition maneuver discussed here is restricted in the longitudinal plane and is assumed to occur in a still atmosphere. The aircraft motion can be formulated as a two-degree-of-freedom point-mass model as follows:

$$m\ddot{x} = T\cos\alpha_{\text{fus}} - D - W\sin\gamma \tag{2}$$

$$m\ddot{z} = L + T\sin\alpha_{\text{fus}} - W\cos\gamma \tag{3}$$

These assumptions simplify the aerodynamics and vehicle dynamics substantially while still providing qualitative, as well as quantitative, insight to the hover-to-cruise transition properties.

In this section, the optimal transition trajectories of varying thrust-to-weight ratios and the mass of the aircraft are analyzed. Additionally, the transition maneuver performances are compared between the conventional fixed-wing configuration (two control variables: thrust and elevator deflection) and the proposed variable-incidence wing 1 configuration (three control variables: thrust, elevator deflection, and angle of incidence of the outboard wing).

The optimal trajectory calculation is based on a fixed-time two-point boundary value problem between the hover and the forward-flight states. The optimal trajectories are evaluated using the commercial nonlinear constrained programming algorithm fmincon, available in the MATLAB® optimization toolbox. The algorithm is based on a sequential quadratic programming technique coupled with a quasi-Newton method, for better efficiency. It has been widely used for nonlinear constrained optimization problems. The input is the initial guess of the variables to be optimized. During each

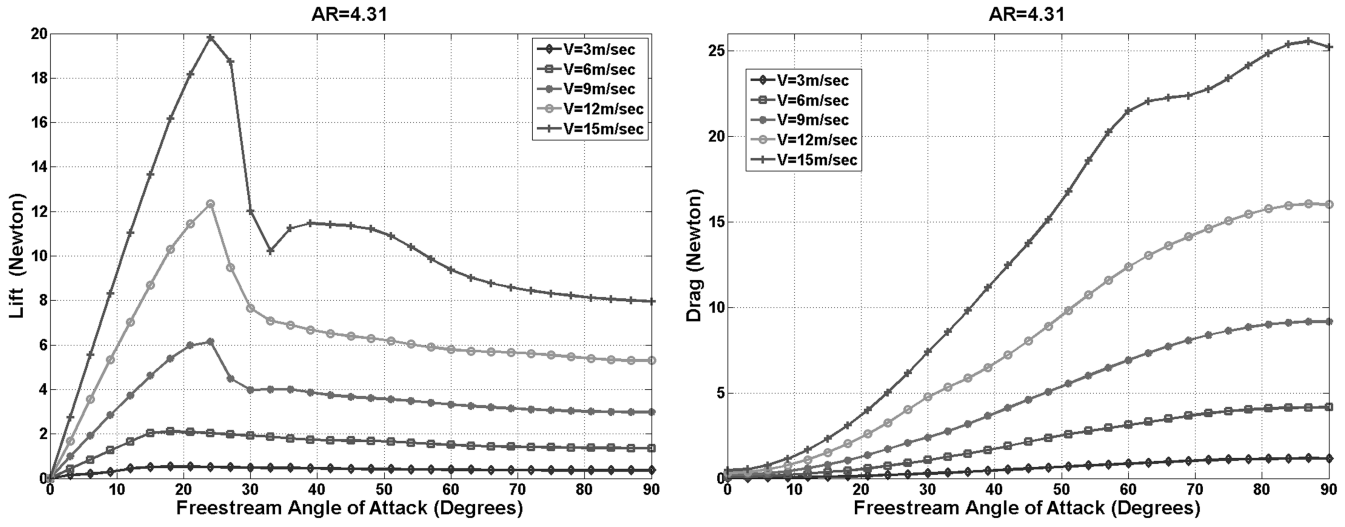

a) b)

Fig. 2 Aerodynamic forces vs AOA for several velocities: a) lift and b) drag.

iteration, the scalar objective function is evaluated, subject to the constraints posed to the dynamics of the vehicle. The output of each iteration is the input for next one. To increase the convergence rate, the initial guess should be in the feasible region near to the optimal output. Global convergence is difficult to attain and is subjected to an initial estimate unless convexity is assumed [14]. The sampling time between two consecutive control inputs is 0.2 s. The classical Runge–Kutta fourth-order method is used for the shooting purpose.

The control variables for the optimization are α_{fus}, α_{wing}, and T, as follows:

$$\mathbf{u} = [\alpha_{\text{fus}} \quad \alpha_{\text{wing}} \quad T]^T \tag{4}$$

For the fixed-wing case, the same control vector can be used by imposing an additional constraint that, at any instant,

$$\alpha_{\text{fus}} = \alpha_{\text{wing}} \tag{5}$$

The objective function for the optimization is based on the mechanical energy formulation [15] as follows:

$$J = w_1 \cdot \frac{1}{2} m|(u_t)^2 - (15)^2| + w_2 \cdot \frac{1}{2} m v_t^2 + w_3 \cdot \left(\sum_{i=1}^{t} |y_i| \right) \tag{6}$$

The first term in the objective function in Eq. (6) indicates the difference in the kinetic energy due to the terminal horizontal velocity and the target horizontal cruise velocity, which are 15 m/s. The second term in Eq. (6) represents the kinetic energy due to terminal vertical velocity, and the third term represents the potential energy. The minimization of the objective function in Eq. (6) indicates the desire to achieve the terminal horizontal target velocity of 15 m/s, with minimum altitude variation during the transition. The weighting factors (w_1, w_2, and w_3) can be adjusted to achieve the desired performance. In this study, the weighting factors used are $w_1 = w_2 = w_3 = 1$, the same for both fixed and variable-incidence wing cases.

The common constraints applied to the dynamics of the vehicle during hover-to-cruise optimization for both the fixed-wing and variable-incidence wing cases are shown in Table 1. The angular rate constraints are included in order to capture the pitching rate limitations, so that the real aircraft dynamics are better represented.

IV. Results and Discussion

A. Optimized Transition Maneuver

A representative case of the optimized transition maneuver is given in Fig. 3, which shows the variable-incidence wing case for the transition time of 4 s. The aircraft position, together with its orientation and the incidence angle of the wing, are plotted at several indicated time instants and airspeeds. It is interesting to note that, during the optimized transition, the angle of incidence of the wing always remains in the prestall regime. A closer observation indicates that the wing incidence stays close to the value that yields maximum lift at the early transition phase and eventually reaches the necessary cruise incidence toward the end. This shows the importance of the variable-incidence wing in assisting the transition aerodynamically to achieve the optimized trajectory. Also note that the optimization scheme leads to the execution of the transition maneuver at a practically constant altitude. These constant-altitude transitions can also be achieved in the fixed-wing case but with a higher T/W and less favorable control histories, as will be discussed in the next sections.

Table 1 Constraints posed to the UAV dynamics for hover-to-cruise optimization

$V \geq 0$	$u_i \geq 0$	$u_i \leq 15$ m/s
$\alpha_{\text{fus}} \geq 0$	$\alpha_{\text{fus}} \leq \frac{\pi}{2}$	$\Delta\alpha_{\text{fus}} \leq 10$ deg/step
$\alpha_{\text{wing}} \geq 0$	$\alpha_{\text{wing}} \leq \frac{\pi}{2}$	$\Delta\alpha_{\text{wing}} \leq 10$ deg/step
$T_i \geq 0.5$	$T_i \leq T_{\max}$	$\Delta T \leq 2N$/step
$\dot{\alpha}_{\text{fus}} \leq 50$ deg/s	$\dot{\alpha}_{\text{wing}} \leq 50$ deg/s	$\dot{T} \leq 4N$/s

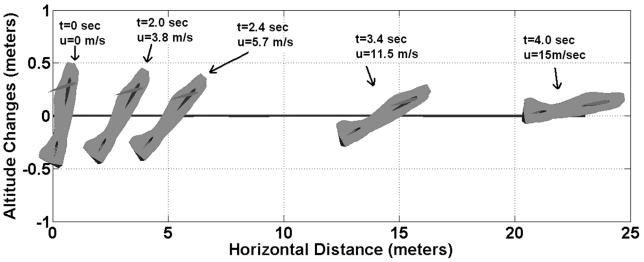

Fig. 3 Optimal 4 s transition for the variable-incidence wing case.

B. Maximum Thrust-to-Weight Ratio Requirements

In Fig. 4, the required $(T/W)_{\max}$ for the constant-altitude transitions is plotted across several masses for both fixed and variable-incidence wing cases. With the increase in the mass of the vehicle, the required $(T/W)_{\max}$ increases for a particular transition time for both cases. This can be explained from the point of view that the transition maneuver is essentially a shift from propulsive-born flight to aerodynamic-born flight. To maintain constant altitude, the following relationship must hold during the maneuver at all instants:

$$\frac{T \sin \alpha_{\text{fus}}}{W} + \frac{L}{W} = 1 \tag{7}$$

As the aerodynamic contribution for L remains unchanged with the increase in W, L/W decreases; therefore, T/W has to increase to satisfy Eq. (7).

Figure 4 also indicates that, with a longer specified transition time, the required $(T/W)_{\max}$ decreases. This trend is similar for different mass values. Moreover, with the use of the variable-incidence wing, the required $(T/W)_{\max}$ is reduced (more so for the shorter transition times). The $(T/W)_{\max}$ value approaches hover thrust as the time allocated for the transition increases. For indoor autonomous UAV application in which such agile maneuvers are carried out under space restrictions, a shorter transition time is very desirable, and with the substantial decrease in the $(T/W)_{\max}$ requirement for a particular mass, the variable-incidence wing feature offers a significant advantage.

C. Control Variations

The control histories for several constant-altitude transition maneuvers at different transition times are plotted in Figs. 5 and 6 for the fixed and variable-incidence wings, respectively. It can be observed that α_{fus} has an almost linear trend for most of the transition time in both cases. Near the end of transition, when the aircraft flight-path angle is small, α_{fus} is almost constant at the cruise value.

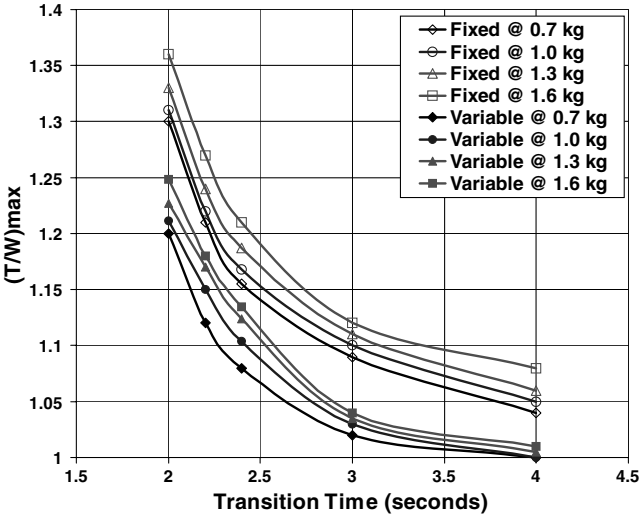

Fig. 4 Effect of mass on $(T/W)_{\max}$ for optimized hover-to-cruise transition for fixed and variable-incidence wing configurations.

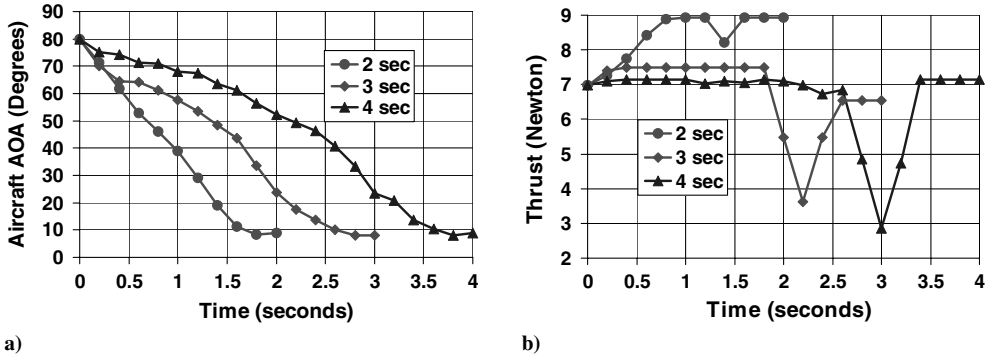

a) b)

Fig. 5 Optimized fixed-wing transitions: a) AOA and b) thrust histories.

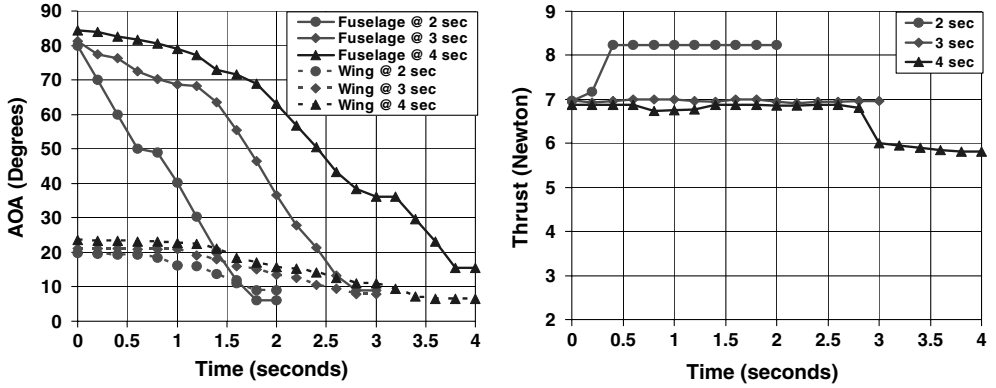

a) b)

Fig. 6 Optimized variable-incidence wing transitions: a) fuselage and wing AOA and b) thrust histories.

For the fixed-wing case, there is a significant dip in the thrust history near the end of the maneuver (Fig. 5b). This trend is observed for the three transition times simulated. This phenomenon is associated with the vehicle's stall properties (see Fig. 2a). As the vehicle starts this maneuver from a trimmed hover condition, which is in the poststall regime, and transitions to lower α_{fus}, the vehicle enters into the prestall regime and results in a significant rise in lift. This sudden increase leads to the immediate decrease in the thrust needed to sustain the horizontal flight path. The needed thrust increases again to achieve the specified terminal flight velocity at the end of the transition.

It can be observed from Fig. 6 that, for the variable-incidence wing case, α_{wing} remains in the prestall regime, such that the outboard wing section poses less drag during the transition and more lift as the airspeed of the aircraft increases. The behavior of α_{fus} is similar to that of the fixed-wing case. As the vehicle picks up speed, α_{wing} reduces to its cruise value near the end of the transition maneuver. As can be observed from the thrust history in Fig. 6b, the dip phenomenon (as in the fixed-wing case) does not appear here because of the sustained aerodynamic contribution of the variable-incidence wing. The outboard wing is in the prestall flow regime for all of the time during the transition and does not cross the stall point (see Fig. 2a). This reduces the variation in thrust, which will potentially reduce the appearance of unwanted dynamics due to the abrupt thrust variation.

V. Conclusions

An aerodynamic-assisted transition technique using a variable-incidence wing has been proposed. The benefits of the variable-incidence wing feature are shown through optimization of the hover-to-cruise transition maneuver for small agile UAVs. The transition performances using the variable-incidence wing have been compared with the conventional fixed-wing configuration. The results reveal the variable-incidence wing advantages in terms of reduced $(T/W)_{\max}$ requirements for a specified transition time and less thrust variations. Moreover, with the increase in mass of the aircraft, the proposed scheme advantage becomes more prominent. Overall, the variable-incidence wing feature is shown to be promising for improving the aircraft transition performance.

References

[1] Pines, D. J., and Bohorquez, F., "Challenges Facing Future Micro-Air-Vehicle Development," *Journal of Aircraft*, Vol. 43, No. 2, 2006, pp. 290–305. doi:10.2514/1.4922

[2] Nieuwstadt, M. J. V., and Murray, R. M., "Rapid Hover-to-Forward-Flight Transitions for a Thrust-Vectored Aircraft," *Journal of Guidance, Control, and Dynamics*, Vol. 21, No. 1, 1998, pp. 93–100. doi:10.2514/2.4202

[3] Stone, R. H., and Clarke, G., "Optimization of Transition Manoeuvres for a Tail-Sitter Unmanned Air Vehicle (UAV)," Australian Aerospace International Congress [online paper], http://www.aeromech.usyd.edu.au/uav/twing/pdfs/AIAC_paper_final.pdf, Paper 105, 2001.

[4] Stone, R., Anderson, P., Hutchison, C., Tsai, A., Gibbens, P., and Wong, K., "Flight Testing of the T-Wing Tail-Sitter Unmanned Air Vehicle," *Journal of Aircraft*, Vol. 45, No. 2, 2008, pp. 673–685. doi:10.2514/1.32750

[5] Osborne, S. R., "Transitions Between Hover and Level Flight for a Tailsitter UAV," Masters of Science Thesis, Brigham Young Univ., Provo, UT, 2007.

[6] Green, W. E., and Oh, P. Y., "A MAV That Flies Like an Airplane and Hovers Like a Helicopter," *Proceedings of the 2005 IEEE/ASME International Conference on Advanced Intelligent Mechatronics*, IEEE Publ., Piscataway, NJ, 2005, pp. 693–698.doi:10.1109/AIM.2005.1511063

[7] Johnson, E. N., Turbe, M. A., Wu, A. D., Kannan, S. K., and Neidhoefer, J. C., "Flight Test Results of Autonomous Fixed-Wing UAV Transitions to and from Stationary Hover," AIAA Paper 2006-6775, 2006.

[8] Frank, A., McGrew, J. S., Valenti, M., Levine, D., and How, J. P., "Hover, Transition, and Level Flight Control Design for a Single-Propeller Indoor Airplane," AIAA Paper 2007-6318, 2007.

[9] Schaefer, C. G., and Baskett, L. J., "GOLDENEYE: The Clandestine UAV," AIAA Paper 2003-6634, 2003.

[10] Kubo, D., and Suzuki, S., "Tail-Sitter Vertical Takeoff and Landing Unmanned Aerial Vehicle: Transition Flight Analysis," *Journal of*

Aircraft, Vol. 45, No. 1, 2008, pp. 292–297. doi:10.2514/1.30122

[11] Hanley, P., MultiSurface Aerodynamics®, MSA Ver. 2.0, Hanley Innovations, Ocala, FL.

[12] Katz, J., *Low Speed Aerodynamics*, Cambridge Univ. Press, New York, 2001.

[13] McCormick, B. W., *Aerodynamics, Aeronautics, and Flight Mechanics*, 2nd ed., Wiley, New York, 1995.

[14] Bonnans, J. F., Gilbert, J. C., Lemarechal, C., and Sagastizabal, C. A., *Numerical Optimization*, 2nd ed., Springer–Verlag, New York, 2006.

[15] Maqsood, A., and Go, T. H., "Study on Aerodynamic Assisted Transition Control Technique for Versatile UAV," AIAA Paper 2009-60, 2009.